Acta Biomaterialia 42 (2016) 168–179

Contents lists available at ScienceDirect

Acta Biomaterialia

journal homepage: www.elsevier.com/locate/actabiomat

Full length article

Anti-inflammatory Chitosan/Poly-γ-glutamic acid nanoparticles control inflammation while remodeling extracellular matrix in degenerated intervertebral disc

Graciosa Q. Teixeira [a,b,c,d], Catarina Leite Pereira [a,b,d], Flávia Castro [a,b,d], Joana R. Ferreira [a,b,d], Maria Gomez-Lazaro [a,b], Paulo Aguiar [a,b], Mário A. Barbosa [a,b,d], Cornelia Neidlinger-Wilke [c], Raquel M. Goncalves [a,b,d,*]

[a] Instituto de Investigação e Inovação em Saúde, Universidade do Porto, Rua Alfredo Allen 208, 4200-135 Porto, Portugal
[b] INEB – Instituto de Engenharia Biomédica, Universidade do Porto, Rua Alfredo Allen 208, 4200-135 Porto, Portugal
[c] Institute of Orthopaedic Research and Biomechanics, University of Ulm, Helmholtzstrasse 14, 89081 Ulm, Germany
[d] ICBAS – Instituto de Ciências Biomédicas Abel Salazar, Universidade do Porto, Rua de Jorge Viterbo Ferreira 228, 4050-313 Porto, Portugal

ARTICLE INFO

Article history:
Received 12 February 2016
Received in revised form 27 May 2016
Accepted 9 June 2016
Available online 15 June 2016

Keywords:
Nanoparticles
Inflammation
Intervertebral disc
Organ culture
Diclofenac

ABSTRACT

Intervertebral disc (IVD) degeneration is one of the most common causes of low back pain (LBP), the leading disorder in terms of years lived with disability. Inflammation can play a role in LPB, while impairs IVD regeneration. In spite of this, different inflammatory targets have been purposed in the context of IVD regeneration.

Anti-inflammatory nanoparticles (NPs) of Chitosan and Poly-(γ-glutamic acid) with a non-steroidal anti-inflammatory drug, diclofenac (Df), were previously shown to counteract a pro-inflammatory response of human macrophages. Here, the effect of intradiscal injection of Df-NPs in degenerated IVD was evaluated. For that, Df-NPs were injected in a bovine IVD organ culture in pro-inflammatory/degenerative conditions, upon stimulation with needle-puncture and interleukin (IL)-1β. Df-NPs were internalized by IVD cells, down-regulating *IL-6*, *IL-8*, *MMP1* and *MMP3*, and decreasing PGE_2 production, compared with IL-1β-stimulated IVD punches. Interestingly, at the same time, Df-NPs promoted an up-regulation of extracellular matrix (ECM) proteins, namely collagen type II and aggrecan. Allover, this study suggests that IVD treatment with Df-NPs not only reduces inflammation, but also delays and/or decreases ECM degradation, opening perspectives to new intradiscal therapies for IVD degeneration, based on the modulation of inflammation.

Statement of Significance

Degeneration of the IVD is an age-related progressive process considered to be the major cause of spine disorders. The pro-inflammatory environment and biomechanics of the degenerated IVD is a challenge for regenerative therapies. The novelty of this work is the intradiscal injection of an anti-inflammatory therapy based on Chitosan (Ch)/Poly-(γ-glutamic acid) (γ-PGA) nanoparticles (NPs) with an anti-inflammatory drug (diclofenac, Df), previously developed by us. This drug delivery system was tested in a pro-inflammatory/degenerative intervertebral disc *ex vivo* model. The main findings support the success of an anti-inflammatory therapy for degenerated IVD that not only reduces inflammation but also promotes native IVD matrix production.

1. Introduction

Pathologies of intervertebral disc (IVD) such as disc degeneration, herniation or cervical radiculopathology are strongly associated with low back pain (LBP) [1,2]. This might be caused by herniation-induced pressure on over-sensitized nerve roots, due to mechanical stimuli, and by molecules arising from the inflammatory cascade [1,3].

In degenerated discs, an up-regulation of metalloproteinases (MMPs) and an over-expression of a wide number of inflammatory mediators (tumor necrosis factor (TNF)-α, interleukin (IL)-1β, IL-6)

* Corresponding author at: Rua Alfredo Allen 208, 4200-135 Porto, Portugal.
E-mail address: raquelg@ineb.up.pt (R.M. Goncalves).

http://dx.doi.org/10.1016/j.actbio.2016.06.013
1742-7061/

have been observed. A balance between inflammatory mediators and their counter-regulatory molecules may be important for determining the immune and regenerative outcome of IVD pathologies [4,5].

Current therapeutic interventions for degenerated IVD are determined by the degree, severity and persistence of pain: conservative approaches, involving rest, pain medication or physiotherapy, in contrast to non-conservative treatments that include microdiscectomy, spinal fusion of two or more disc levels, or disc replacement by prostheses. However, these approaches are only transient and may affect patients' mobility or induce adjacent-level IVD degeneration within few years, leading to chronic low back pain symptoms [2,6].

Therefore, new therapies for degenerative disc disease have been encouraged and intradiscal injection of different molecules has been one of the most appealing strategies. In this context, inflammatory players (including TNF, IL-1 and IL-6) have been suggested as possible targets [5,7]. For example, intradiscal injections of steroids or glucocorticoids are currently performed to decrease intradiscal inflammation in patients with nucleus pulposus-induced spinal nerve root injury [8,9]. Nonetheless, only 25% of success rate has been shown with intradiscal steroid injection at short-term follow-up [10]. At long-term, in patients with chronic LBP, this strategy did not show clinical benefits [11]. Furthermore, intradiscal steroids are thought to promote spinal segment stabilization via further disc degeneration [12].

Non-steroidal anti-inflammatory drugs (NSAIDs), as diclofenac (Df), are considered the most effective anti-inflammatory drugs [13]. These drugs affect the arachidonic acid cascade, inhibiting particularly the cyclo-oxygenase (COX) and lipoxygenase pathways, decreasing inflammation and pain [14,15], and have been widely used in osteoarticular disorders [16]. A local NSAIDs-based therapy would increase drug targeting and bioactivity, while minimizing drug bio-distribution through the organism and the risk of side effects [17].

Different strategies are being investigated to treat degenerated IVD, such as hydrogels for nucleus pulposus replacement, cell-based therapies, growth factors injection or gene therapy [18]. Inflammation is an important aspect of this disorder that is frequently neglected, but its control in the degenerated IVD scenario is crucial for tissue regeneration. Recently, IL-10 and TGF-β anti-inflammatory molecules were described as potential successful therapeutic approaches for the treatment of LBP mediated by IVD degeneration, not only inhibiting inflammation but also, in the case of TGF-β, promoting ECM production [19,20]. Anti-inflammatory NPs have been previously investigated by our group: Chitosan (Ch)/Df/Poly-γ-glutamic acid (γ-PGA) NPs were able to inhibit and revert prostaglandin E_2 (PGE_2) production by activated macrophages *in vitro*, while decreasing IL-6 and partially TNF-α production [17]. So, here we address the effect of these NPs to control inflammation in degenerated IVD. These NPs revealed to be an effective drug-delivery system that can be combined with other strategies as hydrogels to control local inflammation.

Chitosan (Ch) is a natural biodegradable polysaccharide that has been widely used in biomedical applications, mainly in drug delivery systems, gene therapy and tissue engineering [21]. Ch is biochemically active, biocompatible and non-toxic [22]. Previous studies from our group have shown that Ch ultra-thin surfaces polarized macrophages into an M2c phenotype and stimulated dendritic cells, without leading to significant T-cell proliferation [23]. *In vivo*, Ch implants with higher degree of acetylation (DA, 15%) induced a stronger inflammatory reaction, with more extended fibrous capsule and higher number of infiltrated cells [24]. Nevertheless, when Fibrinogen was adsorbed in Ch films, most inflammatory cytokines produced by monocytes/-macrophages were downregulated [25]. Also, when Resolvin D1, a lipid inflammatory mediator, was incorporated into Ch implants, the immune response was almost shut down [26]. Overall, Ch is a versatile biomaterial that can be tuned by its chemistry or protein incorporation to be immunomodulatory [27]. On the other hand, γ-PGA is a naturally occurring peptide that consists of D- and L-glutamic acids polymerized through γ-glutamyl bonds. Contrarily to α-PGA, a counterpart chemically synthesized, γ-PGA is microbially produced by certain Bacillus strains as a capsular or extra-cellular viscous material, is water-soluble, biochemically degraded into glutamate residues and non-toxic [28]. Also, by forming a ternary complex, γ-PGA can be recognized by an intrinsic membrane protein, γ-glutamyl transpeptidase (GGT), resulting in a significant increase in its cellular uptake [28,29].

Ch and γ-PGA are ions with opposite charges that spontaneously self-assemble in a controlled pH environment. The electrostatic interactions between Ch and γ-PGA have been previously explored by our group [22]. Ch/γ-PGA polyelectrolytes are stable at pH 5.0 and have been proposed as delivery systems for different proteins/molecules in different contexts: stromal derived factor-1 [30], interferon-γ [31] and Df [17]. Ch/γ-PGA nanoparticles (NPs) with Df were previously demonstrated to be an effective anti-inflammatory drug delivery system *in vitro* [17].

Therefore, we propose the intradiscal injection of an anti-inflammatory drug delivery system based on Ch/Df/γ-PGA NPs to locally control the inflammatory response in degenerated IVD. For that, a pro-inflammatory/degenerated bovine IVD organ culture model recently established was used [32]. The effect of Ch/Df/γ-PGA NPs specifically on IVD inflammatory markers was here addressed, and also ECM remodeling upon this therapy was evaluated.

2. Materials and methods

2.1. Pro-inflammatory IVD organ culture model and intradiscal anti-inflammatory treatment

Bovine IVDs were isolated from young adult animals' tails (age <48 months old) within 3 h post-slaughter in a local slaughterhouse, with the ethical approval of the Portuguese National Authority for Animal Health. Caudal discs were isolated and cultured according to Teixeira et al. [32]. Briefly, standardized disc punches (with diameter of 9 mm) were collected with nucleus pulposus in the center and few surrounding annulus lamellae and maintained for 6 days in 6-well tissue culture plates, with membrane filter inserts and 0.46 MPa static loading. Basal medium (BM) was Dulbecco's Modified Eagle's Medium with low glucose (DMEM, Biochrom), supplemented with 5% v/v fetal bovine serum (FBS, HyClone), 1% v/v penicillin/streptomycin (10.000 U/mL/10.000 μg/mL, Biowest), 0.5% v/v amphotericin B (Capricorn) and with the osmolarity adjusted to IVD-physiological 400 mOsm by addition of 1.5% v/v of a 5 M NaCl/0.4 M KCl solution. Samples were incubated at reduced oxygen atmosphere (37 °C, 6% O_2 and 8.5% CO_2) and saturated humidity. Culture medium was replaced every second day.

Pro-inflammatory/degenerative stimulation was induced as optimized by Teixeira et al. [32]. Briefly, after 6 days of culture in BM, IVD organ cultures were injured by needle-puncture with a sterile 21-gauge needle and stimulated with pro-inflammatory factor IL-1β (100 ng/mL, PeproTech). Three hours after pro-inflammatory stimulus, discs were treated with injection of 500 μL (corresponding to 10% v/v in solution) of Ch/γ-PGA NPs (0.7 mg/mL), Ch/Df/γ-PGA NPs (0.7 mg/mL) (Df, Sigma-Aldrich) using a microsyringe and a 33-gauge needle (Hamilton). The time point for treatment was selected based on previous work from our team [17,32]. Non-manipulated samples kept in BM were used as

controls. The effects were evaluated 2 days later by gene expression and PGE_2 production quantification. Metabolic activity of the disc cells, tissue DNA and sGAG content and pH of culture supernatants were also analyzed at this time point. For analysis of ECM components at protein level, organ cultures were maintained for 14 days and samples collected for histology. The experimental scheme and groups are represented in Fig. 1.

2.2. Mitochondrial metabolic activity of IVD cells in the organ culture model

To assess cell mitochondrial metabolic activity, resazurin assay was performed. Resazurin (Sigma-Aldrich) stock solution (0.1 mg/mL) was added to IVD culture medium at a final concentration of 10% v/v. Samples were incubated for 3 h at 37 °C. Fluorescence intensity was measured in a spectrophotometer microplate reader (BioTek Synergy HT), with 530 nm excitation filters and 590 nm emission filters. A calibration curve was previously designed to exclude saturated values.

2.3. DNA quantification

DNA content of IVD punches was quantified using Quant-iT PicoGreen double standard DNA (dsDNA) kit (Invitrogen), according to manufacturer's instructions, and normalized to the wet weight of the digested tissue. Tissue digests were obtained by previous incubation of the IVD minced samples with proteinase K (Sigma-Aldrich) solution (0.5 mg/mL in phosphate buffer containing 10.68 g/L $NaH_2PO_4{\cdot}2H_2O$, 8.45 g/L $Na_2HPO_4{\cdot}7H_2O$ and 3.36 g/L Disodium-EDTA in ultrapure water, pH 6.5) overnight at 56 °C.

2.4. Ch/γ-PGA nanoparticles preparation and incorporation of diclofenac

Ch/γ-PGA and Ch/Df/γ-PGA NPs were prepared by co-acervation as previously described by our team [17,33]. Briefly, Ch (France-Chitine) was purified and characterized after purification according to Antunes et al. [22]. Ch with DA of 10.4 ± 1.6% (degree of deacetylation of approximately 89.6%), determined by Fourier transform infrared spectrometry using KBr pellets (FTIR-KBr), and molecular weight (Mw) of 324 ± 27 kDa, determined by size-exclusion chromatography, was used. γ-PGA (Mw of 10–50 kDa; purity level of 99.5%) was microbially produced by *Bacillus subtilis* as described by Pereira et al. [33]. Ch/γ-PGA NPs were prepared at a molar ratio of 1:1.5 (mol Ch:mol γ-PGA) [17]. Solutions of Ch (0.2 mg/mL in 0.2 M AcOH) and γ-PGA (0.2 mg/mL in 0.05 M Tris-HCl buffer with 0.15 M NaCl) were combined by co-acervation method, in which γ-PGA solution was added dropwise to Ch solution, using a 1 mL syringe in a syringe pump (KD Scientific Inc., Holliston, MA), at constant speed (3.6 μL/s) and high stirring at room temperature. The solution's pH was adjusted to 5.0. Df sodium salt (Sigma-Aldrich) solution (10 mg/mL in distilled water) was incorporated in Ch/γ-PGA NPs at a molar ratio of 2:0.35:1.5 (mol Ch:mol Df:mol γ-PGA), according to Gonçalves et al. [17].

2.5. Characterization of Ch/Df/γ-PGA nanoparticles

NPs were characterized concerning their size and polydispersion index (PdI) by dynamic light scattering (DLS, ZetaSizer Nano Zs, Malvern Instruments) as described elsewhere [35]. The calculation used as dispersants the original solutions of γ-PGA (γ-PGA at 0.2 mg/mL in 0.05 M Tris-HCl buffer with 0.15 M NaCl) and Ch (0.2 mg/mL in 0.2 M AcOH), i.e. the solutions where the NPs were formed.

2.6. Preparation of fluorescent Ch and fluorescent Ch/γ-PGA nanoparticles with and without Df

Fluorescent NPs were prepared according to Gonçalves et al. [17]. Briefly, Ch was labeled with fluorescein isothiocyanate (FITC) with 5% of modification (5% of amine groups with FITC), 100 mg of dried Ch were dissolved in 100 mL of 1% v/v AcOH at 4 °C until complete dissolution. FITC (11 mg to achieve 5% modification) was dissolved in 100 mL of methanol. Both solutions (Ch and FITC) were mixed at constant stirring, protected from light, for 3 h. The FITC-labeled Ch (ftCh) was then precipitated with 0.5 M NaOH

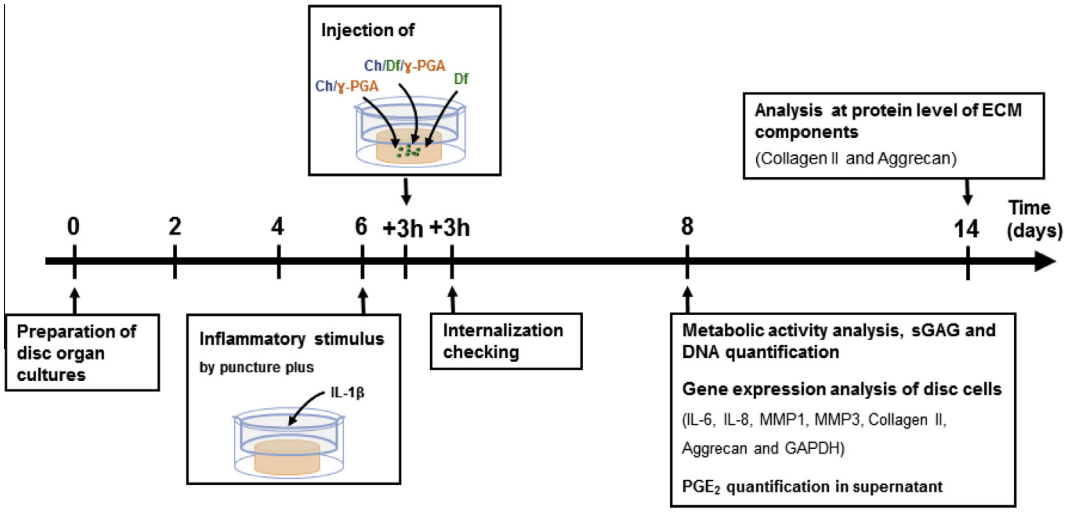

Experimental groups used

Group	Stimulus	Treatment
Control	-	-
IL-1β	puncture plus culture medium supplementation with 100 ng/mL IL-1β	-
NPs		Injection of NPs alone
Df-NPs		Injection of Df-NPs
Df		Injection of soluble Df

Fig. 1. Scheme of the experimental timeline and experimental groups.

and washed with ultrapure water until no fluorescence was seen in the supernatant. ftCh was lyophilized, dried and weighted. ftCh/Df/γ-PGA NPs (Df-ftNPs) were prepared as described above.

2.7. Analysis of internalization of ftCh/Df/γ-PGA nanoparticles by IVD cells using confocal microscopy

Df-ftNPs internalization by IVD cells in the tissue organ culture was analyzed by confocal laser scanning microscopy (CLSM). The Df-ftNPs were injected in disc punches (0.7 mg/mL) as described above. After 1 h of incubation at 37 °C, approximately a 1 mm thickness slice was collected from the center of the disc punch and fixed with 4% v/v paraformaldehyde (PFA). Cells cytoskeleton was stained with Alexa Fluor 594-conjugated Phalloidin (Invitrogen), while cell nuclei were stained with Vectashield with DAPI. The tissue was imaged by CLSM (Leica TCS SP5 AOBS, Leica Microsystems). Z-stacks and orthogonal projections (in XZ and YZ) of single images were analyzed using ImageJ 1.43u software (Wayne Rasband).

2.8. Quantification of ftCh/Df/γ-PGA nanoparticles internalization by IVD cells in the organ culture model

The internalization of Df-ftNPs was quantified by imaging flow cytometry. Disc punches were incubated with Df-ftNPs (0.7 mg/mL) for 3 h. Afterwards, tissue samples were dissected into 2–3 mm^3 fragments and enzymatically digested for 2 h in 1 mg/mL collagenase type I (Sigma-Aldrich) in DMEM, under agitation (50 rpm), reduced oxygen atmosphere (37 °C, 6% O_2 and 8.5% CO_2) and saturated humidity. The supernatant was passed through a 100 μm filter (BD Falcon) to remove tissue debris. Cells were collected by centrifugation at 400*g* for 7 min. The cell suspension was washed once with PBS and fixed in 1% v/v PFA. For imaging flow cytometry (ImagestreamX, Amnis, EDM Millipore), only single cells were used in the analysis, ftCh fluorescence was assessed in Channel 2 (505–560 nm) and at least 2000 events were collected. Image analysis was performed using IDEAS® data analysis software (Amnis). Internalization quantification is described in Supplementary Materials and Methods (S1.1). Briefly, internalization score was calculated based on the ratio of the FITC fluorescence intensity inside the cell and the intensity of the entire cell [34,35]. Higher scores denote larger NPs concentration in the cell cytoplasm, while negative scores denote cells with little internalization.

2.9. Quantitative real-time reverse transcription polymerase chain reaction

Gene expression levels were determined by quantitative real-time reverse transcription polymerase chain reaction (qRT-PCR) on cDNA derived from disc samples. Specific primer pairs were designed using published gene sequences (PubMed, NCBI Entrez Nucleotide Database) and Primer 3 software48 for bovine *IL-6*, *IL-8*, *MMP1*, *MMP3*, collagen type II (*Col II*), aggrecan (*Agg*) and glyceraldehyde 3-phosphate dehydrogenase (*GAPDH*) [32], and synthesized by Alfagene. The analysis was carried out using SYBR Green method. Briefly, IVD punches were digested enzymatically as described above, cell pellets were recovered and total RNA was extracted with ReliaPrep RNA Cell Miniprep System (Promega) according to the manufacturer's instructions. Total RNA was quantified by a NanoDrop spectrophotometer (ND-1000, Thermo) and RNA quality was assessed by means of RNA ratio. Total RNA was reverse transcribed into cDNA using SuperScript® III Reverse Transcriptase kit (Invitrogen). Gene expression levels were determined by qRT-PCR conducted on iQ5 Real-Time PCR Detection System (Bio-Rad), and using iQ™ SYBR® Green Supermix (Bio-Rad). Statistical analysis was performed on ΔC_t values according to a modified method described by MacLean et al. [36]. Fold changes in gene expression were presented as $2^{-(\text{average}\Delta\Delta Ct)}$. The average Ct value of each triplicate measurement of each sample was normalized to the house-keeping gene *GAPDH* in each sample ($\Delta Ct = Ct_{(\text{gene of interest})} - Ct_{(GAPDH)}$). The ΔCt of each stimulated sample was related to the respective ΔCt of each control sample. Normalized values of samples collected at the end of the experiments were compared with the control and between the different experimental groups.

2.10. Prostaglandin E_2 quantification in culture supernatants

Culture medium collected at day 8 was centrifuged (3000 rpm, 5 min) and kept at −20 °C for posterior analysis. PGE_2 was quantified by ELISA (Arbor Assays) according to manufacturer's instructions and normalized by total protein. The bicinchoninic acid colorimetric protein assay was performed according to the manufacturer's instructions (Bio-Rad).

2.11. Sulphated glucosaminoglycans quantification

Sulphated glucosaminoglycans (sGAG) content of IVD punches was assessed at day 8 by reaction with 1,9-dimethyl-methylene blue zinc chloride double salt (DMMB, Sigma-Aldrich) dye reagent solution, containing 40 mM sodium chloride (NaCl, Roth), 40 mM Glycine (Roth) and 46 μM DMMB, previously adjusted to pH 3.0. Chondroitin sulphate A sodium salt from bovine trachea (Sigma) was used as standard. Results were normalized by DNA content.

2.12. Detection of proteoglycans by safranin O/light green staining

IVD punches collected at day 14 of culture were fixed with 4% v/v PFA, processed and embedded in paraffin. Sections of 7 μm thickness were sequentially recovered and stained for safranin O/light green (Saf. O/L. Green, 0.1% v/v Saf. O (Sigma)/0.4% v/v L. Green (Sigma)). Sections were imaged using an Olympus CX31 light microscope equipped with a DP-25 camera (Imaging Software CelÎB, Olympus) using the 20x objective.

2.13. Detection of collagen type II and aggrecan in the IVD

Col II distribution was analyzed by immunofluorescence (IF) staining. Agg production and distribution was analyzed by immunohistochemistry (IHC). For IHC, Novolink™ Polymer Detection Kit (Leica Biosystems) was used, following the manufacturer's instructions. For both, antigen retrieval was performed in paraffin sections through incubation with 20 μg/mL proteinase K (Sigma-Aldrich) solution for 15 min at 37 °C. For Col II staining, after a blocking step, sections were then incubated for 2 h at 37°C with anti-collagen II-II6B3 (Developmental Studies Hybridoma Bank) at a 1:50 dilution. Alexa Fluor 594-labeled goat anti-mouse (Invitrogen-Molecular Probes, 1:1000) was used as secondary antibody. For Agg, sections were incubated overnight with Agg primary antibody (H-300) sc-25674 (Santa Cruz Biotechnology) to a 1:50 dilution.

All sections were mounted in Fluorshield with DAPI (Sigma). Control sections for each labeling excluded primary antibody staining. Representative images of the slides were taken using an inverted fluorescence microscope (Axiovert 200 M, Zeiss) and the 20x objective, for Col II staining. Col II intensity was quantified using a custom-made MATLAB (The MathWorks Inc., Natick MA, USA) script, the IntensityStatisticsMask Software (described in Supplementary Materials and Methods). Agg stained sections were imaged with light microscopy, the 20x objective for counting and the 100x oil objective for detailed imaging.

2.14. Statistical analysis

Results are presented as Median ± Interquartile Range (IQR) in box and whiskers plots. Data normality was first analyzed by D'Agostino and Pearson Normality Test. Statistical analysis was performed with non-parametric Kruskal-Wallis test and Dunns multiple comparison test as post hoc test in Graph Pad v6.02 for Windows. A confidence level of at least 95% ($^*p < 0.05$) was used.

3. Results

3.1. Viability of IVD organ culture model upon Ch/Df/γ-PGA nanoparticles injection

In the present study, we investigated the ability of Df-NPs to revert IL-1β-induced pro-inflammatory stimulus, using an IVD organ culture model previously established [32]. The model closely mimics the IVD inflammatory/degenerative process *in vivo*, for which IL-1β is known to be one of the key mediators [5]. Df-NPs, previously optimized by our group, were able to decrease PGE_2, IL-6 and partially TNF-α production in LPS-activated macrophages [17], thus suggesting that they might be potentially used in other inflammatory scenarios, as in degenerated IVD.

To produce Df-NPs, Df was incorporated in Ch/γ-PGA NPs at a molar ratio of 2.0:0.35:1.5 (Ch:Df:γ-PGA) at pH 5.0, as previously reported [17]. Particle size and PdI of obtained NPs and Df-NPs are summarized in Table 1. The molar ratio, polymer concentration and pH of interaction were first optimized in order to obtain a low poly-disperse solution with nano-size particles of Ch and γ-PGA [33]. Df concentration and its order of addition to those particles were then optimized to guarantee the maximum amount of drug incorporated in the NPs with nano-size and the lowest PdI [17].

The concentration of Df in the NPs was confirmed as previously described, by UV/Vis absorbance (275 nm) of NPs supernatant obtained after NPs centrifugation: about 75% of the initial amount of Df (0.06 mg/mL) was incorporated in Ch/γ-PGA NPs, 1 h after preparation, i.e. Df concentration estimated in the NPs is about 0.045 mg/mL. First, IVD cultures were evaluated concerning their mitochondrial metabolic activity and DNA content, after IL-1β stimulation and treatment with NPs or Df-NPs, to discard possible cytotoxic effects (Fig. 2A and B). Results of the ratio between metabolic activity of disc punches in different conditions and controls showed that IL-1β stimulation slightly increased IVD metabolic activity, which was posteriorly significantly reduced when NPs were injected. In addition, DNA content of IL-1β-treated IVD punches increased significantly, when compared to control discs (1.5 ± 0.5-fold increase, $p < 0.05$). NPs and Df-NPs-treated IVD punches presented similar DNA content to the control (ratios of 0.9 ± 0.4 and 1.0 ± 0.5-fold for NPs-treated/control IVD punches and Df-NPs-treated/control IVD punches in comparison, respectively). Regarding the pH alteration of the cell culture medium upon injection of acidic solutions (NPs and Df-NPs), which might create a toxic or inhibitory environment for the cells, no significant alterations were detected, indicating that the injection of NPs or Df-NPs at pH 5.0 did not significantly acidify the cell culture medium (Fig. 2C).

Table 1
Particle size and polydispersion index of Ch/γ-PGA NPs alone (NPs) and Ch/Df/γ-PGA NPs (Df-NPs).

	Particle size (nm)	Polydispersion index (PdI)	Zeta potential (mV)
NPs	166 ± 32	0.24 ± 0.02	20.8 ± 1.6
Df-NPs	175 ± 32	0.26 ± 0.02	20.5 ± 1.9

3.2. Evaluation of Ch/Df/γ-PGA nanoparticles internalization in IVD organ culture

Imaging of Df-NPs in IVD was performed in inner slices of tissue, as schematically described in Fig. 3A. The fate of Df-NPs in IVD organ culture was evaluated 3 h after Df-NPs injection, in the tissue, by CLSM imaging (Fig. 3B). Df-ftNPs were prepared by previously labeling Ch with FITC, as described by Gonçalves et al. [17]. A broad distribution of NPs within the IVD tissue and partial NPs internalization by IVD cells was observed in randomly selected IVD regions (n = 17 stacks from 3 discs) (Fig. 3B, images a and b). Orthogonal projections in XZ and YZ were performed to evaluate NPs internalization in IVD cells. In those images, we observed that some of Df-ftNPs aggregates were located outside the Phalloidin-stained cell membrane (Fig. 3C, image a, white arrow points Df-ftNPs aggregates), while other Df-ftNPs aggregates were effectively inside the cell (as in Fig. 3C, image b, white arrow points Df-ftNPs aggregates). Therefore, Df-ftNPs internalization was assessed in a high-throughput manner using imaging flow cytometry. First it was determined a viable cell population positive for FITC signal (as shown in Fig. 3D for one donor). By applying a cell mask (Fig. 3E, in blue) and a cytoplasm mask (Fig. 3F, in blue) in the FITC positive cell population, it was possible to determine the internalization ratio between FITC fluorescence intensity inside the cell cytoplasm and FITC fluorescence intensity of the whole cell. This result is depicted for one representative donor in Fig. 3G. Overall,

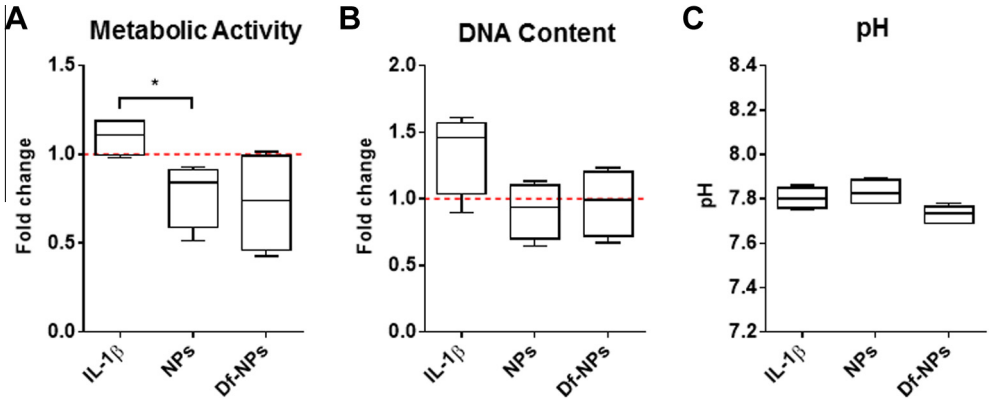

Fig. 2. Viability of the organ culture model, 2 days after pro-inflammatory stimulus with puncture plus IL-1β supplementation (IL-1β), and treatment with injection of Ch/γ-PGA NPs (NPs) or Df/Ch/γ-PGA NPs (Df-NPs). (A) Mitochondrial metabolic activity and (B) DNA content of disc punches. Results were compared with unstimulated IVD organ cultures (control = 1; dashed line). (C) pH of organ culture supernatants for the different conditions. Results are shown as box and whiskers plots (n = 4). $^*p < 0.05$.

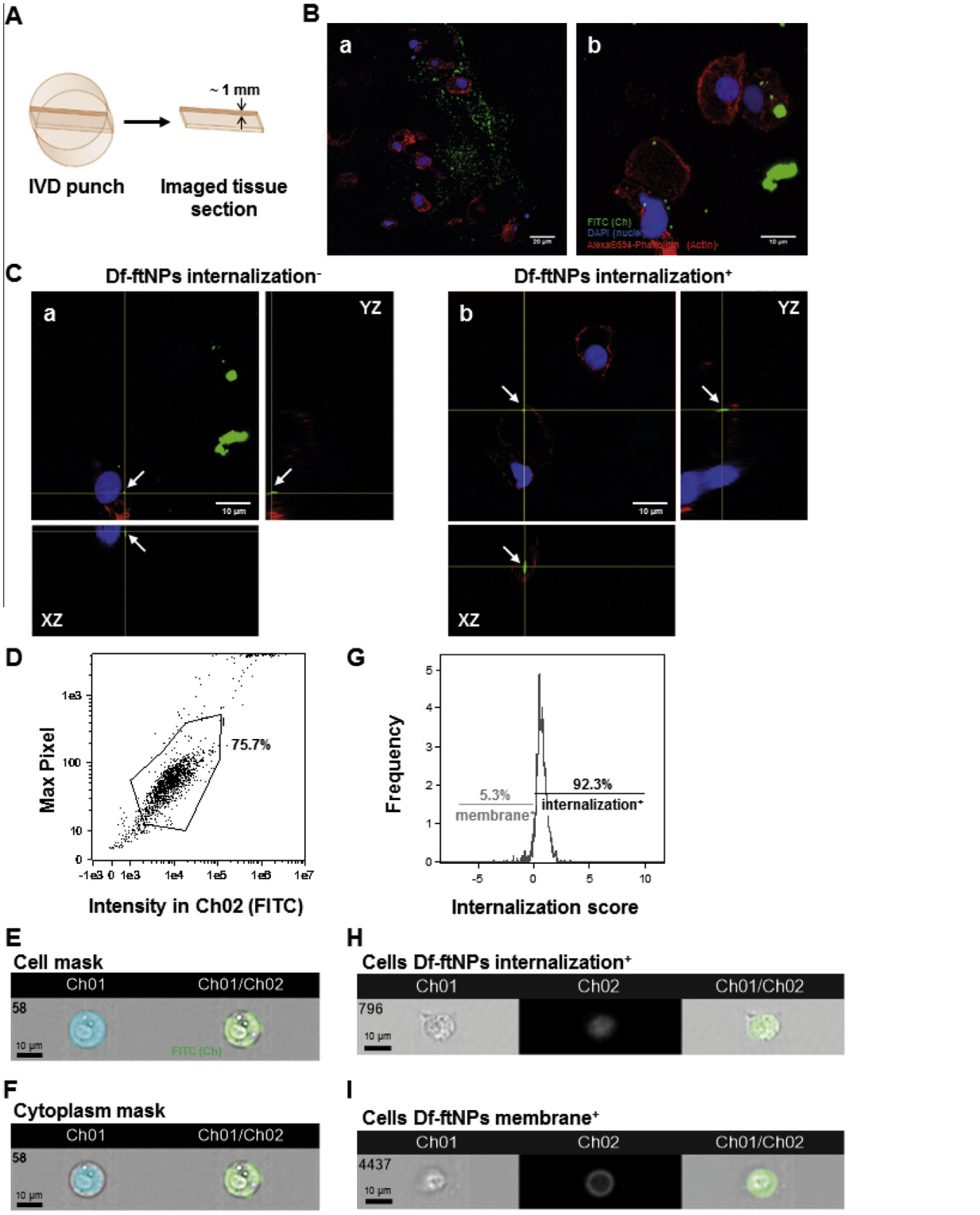

Fig. 3. Internalization of Df-ftNPs by disc cells, after injection treatment of IVD organ cultures, previously stimulated with puncture and IL-1β supplementation. (A) Scheme of tissue collection for image acquisition. (B) Representative CSLM z-projection images of IVD tissue with Df-ftNPs (images a and b; scale bars, 20 μm and 10 μm), acquired 3 h after injection treatment. (C) Orthogonal projections of single images from A (image b) z-projection, showing negative (image a) and positive (image b) cells for Df-ftNPs internalization (white arrow points Df-ftNPs aggregates). Scale bars represent 10 μm. FITC stains the Ch from the Df-ftNPs in green, Alexa®594-Phalloidin stains F-actin in red and DAPI stains nuclei in blue. (D) Representative dot plot profile for the Df-ftNPs internalization analysis. Internalization was assessed by FITC fluorescence in Channel 2 (Ch02). (E) Cell mask (in blue). (F) Cytoplasm mask (in blue). (G) Representative internalization score histogram, after application of an internalization mask in the population of positive cells for Df-ftNPs (Df-ftNPs^{+}). (H) Positive cells for Df-ftNPs internalization (internalization^{+}). (I) Cells with higher fluorescence on the cell membrane compared to the cytoplasm (membrane^{+}). Each cell is represented by a row of three images acquired simultaneously in flow, from left to right: brightfield (gray), FITC fluorescence (green) from the Df-ftNPs, merged image (scale bars, 10 μm) (n = 4). (For interpretation of the references to colour in this figure legend, the reader is referred to the web version of this article.)

about 92 ± 1% of viable cells presented higher FITC fluorescence in the cytoplasm (Fig. 3H), represented by a positive value of the internalization score, thus being Df-ftNPs internalization$^+$ cells. On the other hand, 6 ± 1% of viable cells presented higher fluorescence intensity in the cell membrane (Fig. 3I), represented by a negative value of the internalization score, meaning that in these cells Df-NPs were mostly not internalized (Df-ftNPs membrane$^+$ cells).

3.3. Anti-inflammatory potential of Ch/Df/γ-PGA nanoparticles injection in pro-inflammatory/degenerative IVD organ culture model and evaluation of ECM remodeling

In the IVD organ culture model previously established, the up-regulation of the inflammatory markers *IL-6*, *IL-8* and PGE_2 obtained in pro-inflammatory conditions was reverted by intradiscal injection of Df [32]. Therefore, the efficacy of Df-NPs was first evaluated by assessing the expression of *IL-6* and *IL-8* by IVD cells, and by quantification of PGE_2 in culture medium, 2 days after treatment. MMPs and main ECM proteins of the pro-inflammatory/degenerated IVD *ex vivo* model were also analyzed 2 days post-treatment with Df-NPs. The results are presented as the Median ± IQR fold change to unstimulated IVD punches (Fig. 4).

In the present work, the injection of Df-NPs was able to significantly decrease PGE_2 (∗∗, $p < 0.01$) and down-regulate *IL-6* (∗, $p < 0.05$) when compared to IL-1β-stimulated group (Fig. 4A and B). Df-NPs also seemed to decrease *IL-8* of IL-1β group (from 19 ± 25-fold to 4 ± 7-fold). These values correspond to a reduction of about 73%, 61% and 78% for *IL-6*, PGE_2 and *IL-8*, in relation to IL-1β-stimulated discs. In parallel, control injections with NPs (without anti-inflammatory drug) were also performed. The injection of NPs by itself also reduced *IL-8* expression and PGE_2 production, although no significant differences were observed (reduction to 12 ± 16-fold and 4 ± 2-fold for *IL-8* and PGE_2, respectively), representing approximately a reduction of 35% and 61% when compared to IL-1β group.

Df intradiscal injection was previously shown to down-regulate *MMP1* and up-regulate *Agg* gene expression levels, but no significant effects in *MMP3* and *Col II* levels were observed [32]. In this study, Df-NPs were able to significantly down-regulate both *MMP1* and *MMP3* gene expression (∗∗, $p < 0.01$, Fig. 4C). In addition, NPs alone significantly decreased *MMP3* (∗, $p < 0.05$) and slightly down-regulated *MMP1* (from 5 ± 4-fold, for IL-1β group, to 2 ± 4-fold). These results represent a down-regulation of approximately 63% and 40% for *MMP1* and *MMP3 genes*, respectively. Concerning ECM proteins (Fig. 4D), *Col II* and *Agg* were significantly up-regulated upon Df-NPs treatment (∗, $p < 0.05$ and ∗∗, $p < 0.01$, for Col II and Agg, respectively) in IL-1β-treated IVD punches. Interestingly, NPs group by itself also up-regulated *Agg* expression (∗∗, $p < 0.01$) and increased *Col II* (from 0.1 ± 0.2 of IL-1β-IVDs to 0.2 ± 0.4 of NPs-IVDs). These results represent an increase of about 45% and 85% for *Col II* and *Agg* gene expression, in relation to IL-1β.

3.4. Evaluation at protein level of ECM remodeling in longer-term pro-inflammatory IVD organ culture upon treatment with Ch/Df/γ-PGA NPs

To confirm the effects of these different treatments at protein level, the IVD organ cultures were maintained for 14 days, after which Col II and Agg deposition were analyzed by histology/IHC. A group injected with soluble Df (19 μm) was added, since previous results only showed the effect of soluble Df at gene expression

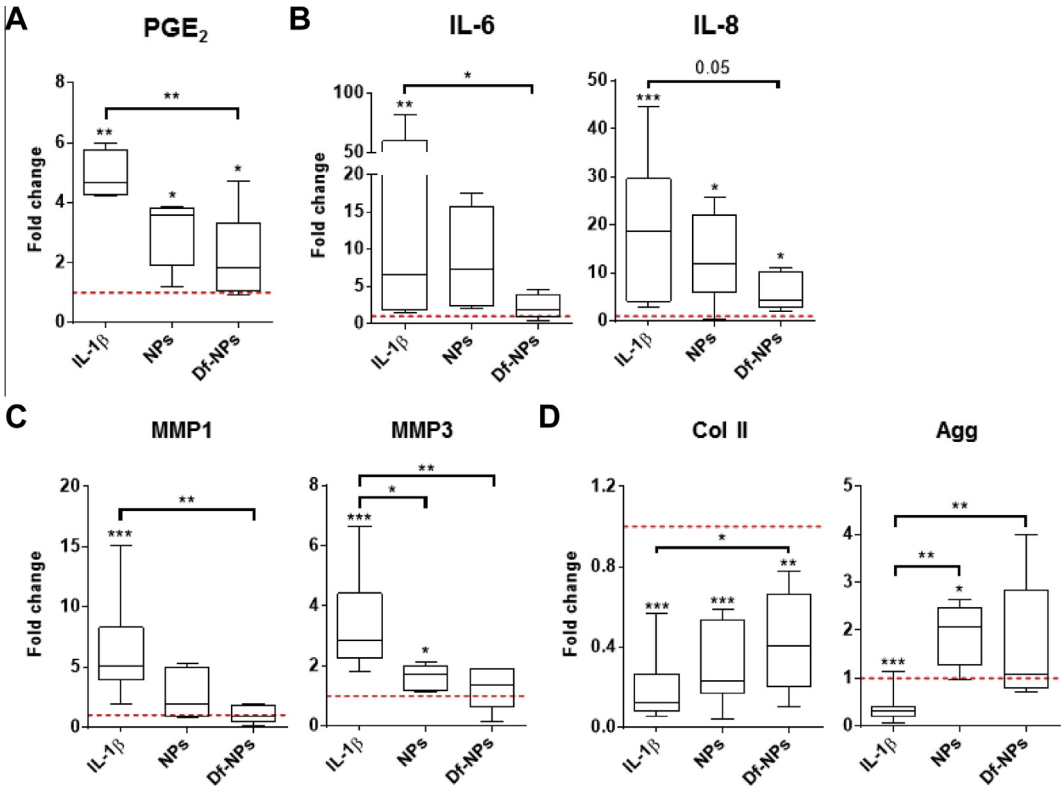

Fig. 4. Effect of different injectable treatments in the inflammatory response and in the ECM remodeling of IVD organ culture pro-inflammatory/degenerative model, 2 days after injection. Quantitative analysis of pro-inflammatory markers of IVD organ cultures stimulated with puncture and IL-1β supplementation (IL-1β), and treated with injection of NPs or Df-NPs. (A) PGE_2 fold change in culture supernatants. (B) mRNA expression of *IL-6*, *IL-8*, (C) matrix degrading enzymes *MMP1* and *MMP3*, and (D) ECM components *Col II* and *Agg*. mRNA levels were normalized to *GAPDH* control gene and to the unstimulated discs (control level = 1; dashed line). Results are presented as box and whiskers plots (n = 6–19). $^*p < 0.05$; $^{**}p < 0.01$; $^{***}p < 0.001$.

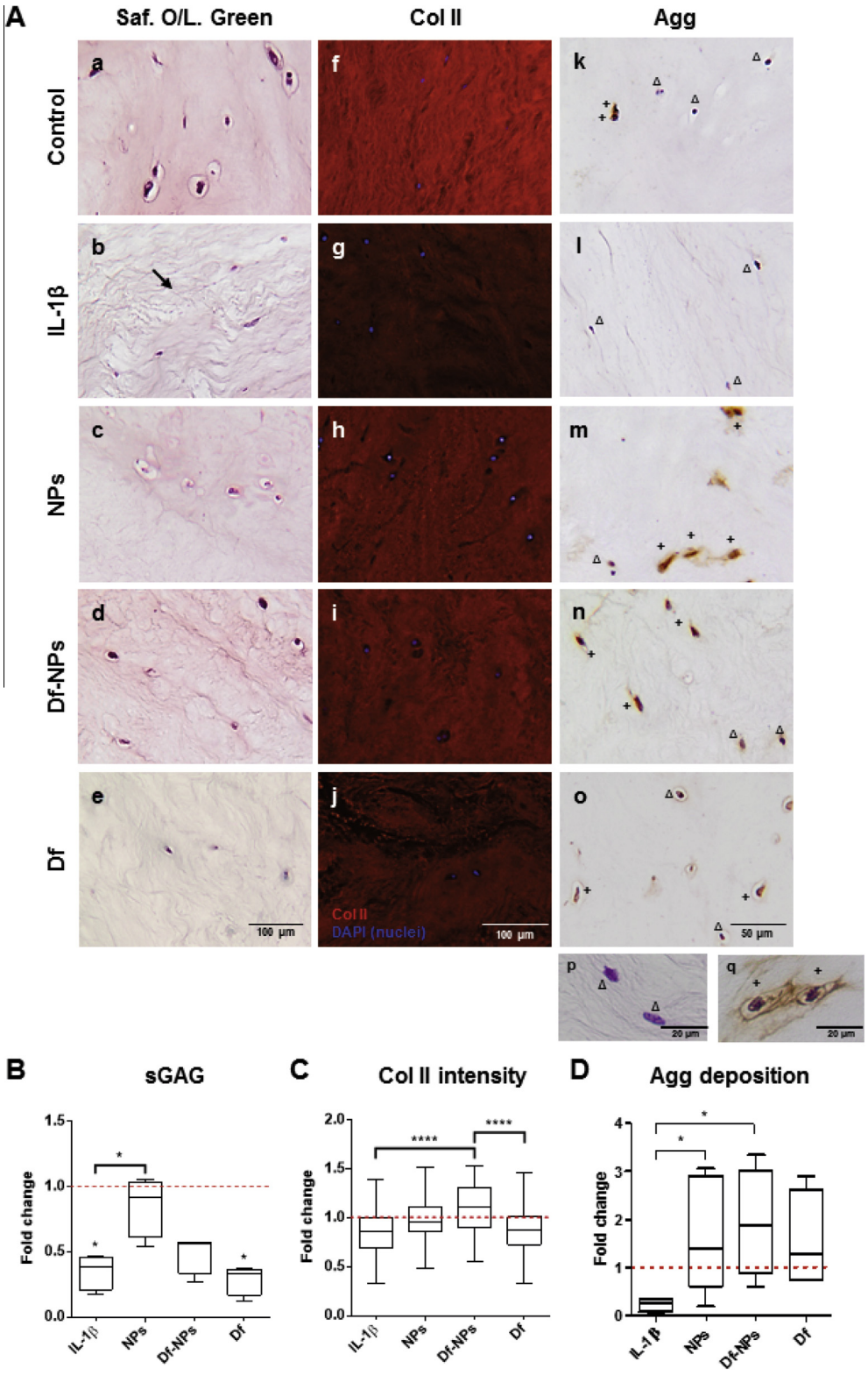

Fig. 5. Effect of different injectable treatments in the ECM of IVD pro-inflammatory/degenerative organ culture model, at the protein level. (A) Sagittal sections of disc punches stained for proteoglycans (a–e; scale bar, 100 µm), Col II (f–j; scale bar, 200 µm), Agg (k–o; scale bar, 100 µm) and higher magnification of Agg negative (p, Agg^-, Δ) and positive (q, Agg^+, +) cells (scale bars, 10 µm). Samples were collected after a 14-days culture. One representative experiment of 3–4 different donors is presented here. (B) Biochemical analysis of sGAG content of IVD punches, at day 8 of organ culture, normalized to control (n = 4 donors). (C) Col II fluorescence intensity normalized to control (dashed line; n = 65–98 from 4 donors), at day 14 of culture. (D) Fold change in % of Agg^+ cells normalized to control group (n = 4 donors), at day 14 of culture. Results are shown as box and whiskers plots (B–D). $^*p < 0.05$; $^{****}p < 0.0001$.

level [32]. Fig. 5A (images a–e) shows Saf. O/L. Green-stained sections of IVD nucleus pulposus for all conditions tested. The control group seemed to exhibit a more compact matrix, with cells and the respective lacunae perfectly contained within the matrix, while in the remaining conditions a higher disorganization in the fibers arrangement was observed, namely in IL-1β condition (Fig. 5A,

image b, arrow). Quantification of disc punches (nucleus pulposus containing few surrounding annulus) sGAG content was performed at day 8 of culture. IL-1β and Df presented a lower concentration of sGAG in tissue, when compared to the control, as shown in Fig. 5B. On the other hand, NPs-treated group presented a significantly higher sGAG content relatively to IL-1β-stimulated group (∗, $p < 0.05$).

Col II and Agg deposition were assessed by IHC. Fig. 5A (images f–j) shows images of Col II staining of all the conditions tested. There were collected 65–98 images from randomly selected areas of each section and samples were collected from 4 different donors. Col II fluorescence intensity was quantified in the IntensityStatisticsMask Software and is depicted as fold change to unstimulated IVD punches in Fig. 5C. The results obtained display significantly higher Col II deposition in Df-NPs group, in comparison with the IL-1β-stimulated samples (∗∗∗∗, $p < 0.0001$). This was not observed in NPs and in Df groups.

In Fig. 5A (images k–o) it is also shown Agg deposition (brown) for the different conditions analyzed (images p and q portray in higher magnification cells negative (Agg^-, Δ) and positive (Agg^+, +) for Agg production). Since Agg deposition was located only around the cells, the numbers of Agg^+ and Agg^- cells were quantified (Fig. 5D). In Fig. 5D it is depicted the fold change of the % of Agg^+ cells (normalized to control group), for 4 different donors. The results obtained show that IVD treatments with NPs and Df-NPs significantly increased the percentage of Agg^+ cells, compared to IL-1β-stimulated discs, when normalized to control group (∗, $p < 0.05$).

4. Discussion

This study hypothesizes that local control of inflammation in degenerated IVD could improve ECM remodeling, which would improve LBP symptoms, constituting a more effective intradiscal therapy. Pro-inflammatory cytokines, TNF-α and IL-1β, are known to induce the expression of genes encoding MMPs, and also induce nucleus pulposus cells to secrete innervation and angiogenic growth factors when the balance between human IVD anabolism and catabolism is disrupted. MMPs degrade both collagen and proteoglycans, leading to tissue dehydration and progressive ECM disorganization. With increasing time, Col II in the nucleus pulposus is replaced by Col I, and the anatomical border between nucleus pulposus and annulus fibrosus becomes less defined, with the nucleus becoming more fibrotic [37].

For that, a pro-inflammatory/degenerative organ culture model, with 0.46 MPa static loading, tissue needle punctured and stimulated with IL-1β (100 ng/mL) was used upon previous validation [32]. This model mimics human IVD degeneration, in which pro-inflammatory cytokines TNF-α and IL-1β are key mediators [5,38]. In this model, an up-regulation of pro-inflammatory markers (*IL-6*, *IL-8*, *MMP1* and *MMP3*), as well as a down-regulation of ECM proteins (*Col II* and *Agg*) was observed [32], in accordance to findings reported during human disc degeneration [5,38].

Although organ cultures as this model are accepted as more reliable models than 2D *in vitro* cultures, constituting an important step before animal experimentation, they have some limitations. One of these includes time in culture to guarantee tissue viability (usually up to 1 week) [39–41]. Here, tissue viability maintenance was monitored by mitochondrial metabolic activity and DNA content. Other studies had already reported high cell viability in IVD organ cultures in pro-inflammatory conditions after 7 [32] and 14 days [42]. Nonetheless, needle insertion can cause cell damage [40], as well as an increase in cell apoptosis after IL-1β treatment [43]. Also, cell viability upon intradiscal injection in acidic conditions (with NPs) was not significantly affected. Another limitation of the organ culture model is the lack of vascularization/innervation (and immune cells) in the disc surroundings. Nevertheless, in this case the lack of complexity constitutes an important advantage when analyzing the direct effect of an intradiscal therapy on IVD cells, without the complex cell crosstalk that we find *in vivo*.

As previously discussed, intradiscal steroid therapy has been adopted by patients with symptomatic disc degeneration and low back pain, unwilling to accept surgical procedures [10,44]. However, placebo-controlled studies about intradiscal steroid injections for discogenic pain have reported either no clinical improvement compared to placebo [11] or short-term improvement [10]. Furthermore, their influence on deregulation of matrix turnover promotes disc degeneration [8]. Also, an increase in the frequency and dosage of intradiscal steroid injections may further accelerate it through puncture injury [44].

Df reduced nucleus pulposus-induced nerve root dysfunction after 7 days of treatment [15]. In the pro-inflammatory/degenerated IVD *ex vivo* model previously established by us, Df injection down-regulated *IL-6*, *IL-8* and decreased PGE_2 production, and also seemed to have an effect in IVD ECM remodeling by down-regulating *MMP1*, while up-regulating *Agg* expression [32].

Nonetheless, Df intraperitoneal injection in a rat lumbar disc herniation model showed a reduced analgesic effect with time [45]. Therefore, Df direct injection into the IVD may have a limited long-term clinical use as it has a short biologic half-life and may require repeated administrations [32].

In this study, we hypothesize that a Df delivery system based on Ch/γ-PGA NPs could extend Df action, controlling inflammation while contributing to ECM remodeling in degenerated IVD. Therefore, Df-NPs were tested as an anti-inflammatory therapy for degenerated IVD.

Small-scale particles are emerging as delivery systems for IVD regeneration. NPs size enables them to pass through biological barriers, having the possibility to be internalized into target cells [46]. Moreover, NPs can be easily combined with hydrogels for cell delivery or nucleus pulposus regeneration, increasing the functionality of biomaterials for IVD [47,48]. Examples of NPs are fullerol NPs (approximately 25–50 nm size) that decreased IVD degeneration in human cells and rabbits [49]. NPs are low viscous vehicle, thus easy to inject into the IVD. Moreover, Ch/γ-PGA NPs were recently shown to promote Col II production in nucleotomized IVD model [50]. Df-NPs are a monodisperse population of NPs that release Df within 2 h in physiological pH (maximum of 80%) [17,33]. In this study, Df-NPs were injected in IVD organ cultures 3 h after the pro-inflammatory stimulus. This time point was selected based in previous work using LPS-activated macrophages, after which PGE_2, the Df target, started to be released to the culture medium [17]. NPs internalization by IVD cells was verified, showing that about 65 ± 6% of tissue total cells contained NPs, corroborating the phagocytic activity of nucleus pulposus cells previously suggested [50,51]. The mechanism of intracellular trafficking of these NPs was not specifically addressed, but others have already investigated the intracellular fate of Ch/γ-PGA NPs. Peng et al. showed that Ch/DNA/γ-PGA NPs can be internalized by specific trypsin-cleavable proteins [52], and by a lipid raft-mediated route, and via macropinocytosis, in a minor extent [29]. Moreover, these authors have shown that when γ-PGA is present in Ch/DNA NPs, less percentage of NPs co-localization with lysosomes, is observed, suggesting that γ-PGA can escape this defense mechanism [29].

Df-NPs decreased *IL-6*, *IL-8* and PGE_2 production, indicating that Df released from the NPs maintained its ability to inhibit COX-2 pathway, as expected [15], and similarly to what was observed with Df injection [32]. NPs, with and without Df, were shown to affect macrophage functional behavior *in vitro*, by stimulating the production of IL-6, IL-10, TNF-α but not IL-12/23, while PGE_2 was only stimulated by NPs without Df [17]. Weather Df-NPs influence

macrophage behavior in degenerated IVD will be addressed in the future.

The promising results of Df-NPs regarding the reduction of pro-inflammatory markers in the ex vivo model do not exclude the need to perform more studies in order to conclude about the feasibility of this therapy, namely testing *in vivo* different times and dosages of NPs administration before moving to pre-clinical research. Although this model aims to mimic some typical features of human IVD degeneration by up-regulating pro-inflammatory mediators, MMPs and down-regulating ECM proteins [32], it cannot fully simulate the native process of chronic IVD degeneration, as naturally occurring in humans and in other species as chondrodystrophic dogs [53] or the sand rat [54]. Nevertheless, these models also have some drawbacks: first, the rat/dog IVD contains notochordal cells, which do not occur in human adults or bovine IVD; second, the long waiting time to observe spontaneous IVD degeneration; and third, the lack of control of this process, which discourages the use of these models [53,54].

Concerning ECM remodeling, previous studies have demonstrated that Df injection was able to decrease *MMP1* and increase *Agg* expression [32]. Interestingly, NPs by itself down-regulated *MMP3* (but not *MMP1*) expression, while Df-NPs down-regulated the expression of both *MMP1* and *MMP3* compared to IL-1β-stimulated discs. In the case of ECM proteins, NPs alone significantly upregulate *Agg* expression, while Df-NPs significantly increase both *Col II* and *Agg* gene expression levels. This result was confirmed at the protein level.

These results support previous evidences from our group, demonstrating that γ-PGA promotes chondrogenesis of MSCs *in vitro*, enhancing Col II, Agg and Sox-9 early expression [55]. This effect was partially observed in IVD organ cultures [50]. In addition, γ-PGA injections have already been patented for treating joint pain [56]. Nevertheless, Ch/γ-PGA NPs mechanism behind chondrogenesis/cartilage formation remains to be explored. The concentration of γ-PGA used in this study was in accordance with previous work from our group [17,22,30,31,33,50]. Nevertheless, in the literature several studies have been used γ-PGA to elicit immune response: about 2.7 mg/mL of γ-PGA with different Mw (from 10 to 2000 kDa) were orally administered inducing significant NK-cell-mediated anti-tumor immunity in mice [57]. Other study administered 5 mg/mL of γ-PGA in mice, inducing antiviral activity and protective immune responses against H1N1 influenza-A virus infection [58]. Another frequent use of γ-PGA is as adjuvant in cancer treatment, by combination with chemotherapeutic agents. γ-PGA NPs were shown to activate dendritic cells usually in high concentrations (10 mg/mL) [59,60]. To the best of our knowledge, the concentrations administered are slightly higher than ours.

Previous studies demonstrate that Ch/γ-PGA NPs are able to infiltrate cell-cell junctions [61,62] and that internalization of Ch/γ-PGA NPs might occur mainly via non-specific charge-mediated interaction (NPs positive charge vs negative charged cell membrane) [52]. Further studies found that Ch/DNA/γ-PGA internalization take place via macropinocytosis and caveolae-mediated pathway, with the latter playing a major role [29]. On the other hand, γ-PGA-coated complexes can be internalized via a specific γ-glutamyltransferase (GGT)-mediated pathway [28,63]. The results obtained in this study suggest the involvement of MMP3, but not MMP1, in the IVD ECM remodeling mediated by Ch/γ-PGA complexes. Moreover, the synergy between Df and Ch/γ-PGA NPs suggests that control of inflammation in degenerated IVD is essential for Col II, but not for Agg production. In fact, this observation was reported in other models described in the literature [20,64]. PGE_2 (10 pg/mL)-stimulated osteoarthritic cartilage-explant cultures cleavage of Col II was downregulated, while no effect was observed in Agg production [64]; in MSCs/nucleus pulposus cells co-cultures, inhibition of TGF-β1 profoundly constrained Col II production, while Agg synthesis was only slightly inhibited, suggesting a crucial role of TGF-β in Col II production in the nucleus pulposus [20]. Nevertheless, to our knowledge this relation is not straightforward, since other authors have suggested that Agg production is also dependent on inflammation control and that TGF-β1 may be also involved. Treatment of (TNF-α + IL-1β)-stimulated annulus fibrosus cells with TGF-β1 and BMP-2 showed a synergic action of both proteins in recovering degenerated IVD ECM: a high increase in Agg gene expression was observed after TGF-β1-treatment, while a high increase in Col II was observed with BMP-2 treatment. Overall, when treated with TGF-β1 + BMP-2, an increase in both Agg and Col II was observed [65].

Nevertheless, future studies will be necessary to highlight the molecular mechanisms behind Ch/Df/γ-PGA NPs-driving effect in degenerated IVD and confirm the hypothesis of a MMP3-mediated stimulation of ECM production in the disc.

5. Conclusions

Intradiscal injection of Ch/Df/γ-PGA NPs reduced pro-inflammatory mediators (*IL-6*, *IL-8* and PGE_2) in a pro-inflammatory/degenerative IVD organ culture model. This anti-inflammatory delivery system also down-regulated the expression of both *MMPs 1* and *3*, while up-regulated Col II and Agg production. Overall, this study suggests that Ch/Df/γ-PGA NPs injection is a promisor intradiscal therapy for degenerated IVD repair/regeneration. This work provides a solid base for testing intradiscal injection of Ch/Df/γ-PGA NPs *in vivo* in an animal model. Although Df has a limited long-term clinical use, as it has a short biologic half-life, we hope to decrease Df administration rates with this strategy and contribute to sustain the native ECM production in patients with discogenic pain. Moreover, the versatility of Ch/γ-PGA NPs allows its combination with other therapies.

Disclosure

The authors declare no competing financial interests.

Acknowledgements

The authors of the present study wish to thank Carnes Landeiro, SA, for kindly providing the bovine tails, Susana Santos and Ana H. Lourenço for the assistance with CSLM, Inês Almeida for the help with qRT-PCR, Daniela Vasconcelos for the help with samples preparation, and also to Helga Bach and Iris Baum for their excellent technical assistance.

This work was financed by Portuguese funds through FCT – Fundação para a Ciência e a Tecnologia in the framework of project UID/BIM/04293/2013. Graciosa Q. Teixeira, Catarina L. Pereira, Flávia Castro and Raquel M. Gonçalves acknowledge FCT for their grants (PhD grants SFRH/BD/88429/2012, SFRH/BD/85779/2012 and PD/BD/114013/2015, for Graciosa, Catarina and Flávia, respectively) and FCT Investigator Starting Grant (IF/00638/2014 for Raquel). The authors would also like to acknowledge the German Spine Foundation (Deutsche Wirbelsäulenstitung), the German Academic Exchange Service (DAAD), the EuroSpine Task Force, and the Conselho de Reitores das Universidades Portuguesas (CRUP).

Appendix A. Supplementary data

Supplementary data associated with this article can be found, in the online version, at http://dx.doi.org/10.1016/j.actbio.2016.06.013.

References

[1] M.A. Adams, P. Lama, U. Zehra, P. Dolan, Why do some intervertebral discs degenerate, when others (in the same spine) do not?, Clin Anat. 28 (2014) 195–204.

[2] F.M. Phillips, P.J. Slosar, J.A. Youssef, G. Andersson, F. Papatheofanis, Lumbar spine fusion for chronic low back pain due to degenerative disc disease: a systematic review, Spine 38 (2013) E409–E422.

[3] E.I. de Schepper, J. Damen, J.B. van Meurs, A.Z. Ginai, M. Popham, A. Hofman, B. W. Koes, S.M. Bierma-Zeinstra, The association between lumbar disc degeneration and low back pain: the influence of age, gender, and individual radiographic features, Spine 35 (2010) 531–536.

[4] C.L. Le Maitre, J.A. Hoyland, A.J. Freemont, Interleukin-1 receptor antagonist delivered directly and by gene therapy inhibits matrix degradation in the intact degenerate human intervertebral disc: an in situ zymographic and gene therapy study, Arthritis Res. Ther. 9 (2007) R83.

[5] M.V. Risbud, I.M. Shapiro, Role of cytokines in intervertebral disc degeneration: pain and disc content, Nat. Rev. Rheumatol. 10 (2014) 44–56.

[6] P.P. Raj, Intervertebral disc: anatomy-physiology-pathophysiology-treatment, Pain Pract. 8 (2008) 18–44.

[7] M. Molinos, C.R. Almeida, J. Caldeira, C. Cunha, R.M. Gonçalves, M.A. Barbosa, Inflammation in intervertebral disc degeneration and regeneration, J. R. Soc. Interface 12 (2015) 20141191.

[8] J.M. Berthelot, B. Le Goff, Y. Maugars, Side effects of corticosteroid injections: what's new?, Joint Bone Spine 80 (2013) 363–367

[9] L. Manchikanti, M.V. Boswell, S. Datta, B. Fellows, S. Abdi, V. Singh, R.M. Benyamin, F.J. Falco, S. Helm, S.M. Hayek, H.S. Smith, Comprehensive review of therapeutic interventions in managing chronic spinal pain, Pain Physician 12 (2009) E123–E198.

[10] G.R. Buttermann, The effect of spinal steroid injections for degenerative disc disease, Spine J. 4 (2004) 495–505.

[11] A. Khot, M. Bowditch, J. Powell, D. Sharp, The use of intradiscal steroid therapy for lumbar spinal discogenic pain: a randomized controlled trial, Spine 29 (2004) 833–837.

[12] S. Muzin, Z. Isaac, J. Walker 3rd, The role of intradiscal steroids in the treatment of discogenic low back pain, Curr. Rev. Musculoskelet. Med. 1 (2008) 103–107.

[13] M. Dougados, Why and how to use NSAIDs in osteoarthritis, J. Cardiovasc. Pharmacol. 47 (2006) S49–54.

[14] M. Kato, S. Nishida, H. Kitasato, N. Sakata, S. Kawai, Cyclooxygenase-1 and cyclooxygenase-2 selectivity of non-steroidal anti-inflammatory drugs: investigation using human peripheral monocytes, J. Pharm. Pharmacol. 53 (2001) 1679–1685.

[15] M. Cornefjord, K. Olmarker, K. Otani, B. Rydevik, Nucleus pulposus-induced nerve root injury: effects of diclofenac and ketoprofen, Eur. Spine J. 11 (2002) 57–61.

[16] F. Richy, O. Bruyere, O. Ethgen, V. Rabenda, G. Bouvenot, M. Audran, G. Herrero-Beaumont, A. Moore, R. Eliakim, M. Haim, J.Y. Reginster, Time dependent risk of gastrointestinal complications induced by non-steroidal anti-inflammatory drug use: a consensus statement using a meta-analytic approach, Ann. Rheum. Dis. 63 (2004) 759–766.

[17] R.M. Gonçalves, A.C.L. Pereira, I.O. Pereira, M.J. Oliveira, M.A. Barbosa, Macrophage response to chitosan/poly-(γ-glutamic acid) nanoparticles carrying an anti-inflammatory drug, J. Mater. Sci. Mater. Med. 26 (2015) 167–178.

[18] D. Sakai, G.B. Andersson, Stem cell therapy for intervertebral disc regeneration: obstacles and solutions, Nat. Rev. Rheumatol. 11 (2015) 243–256.

[19] W. Li, T. Liu, L. Wu, C. Chen, Z. Jia, X. Bai, D. Ruan, Blocking the function of inflammatory cytokines and mediators by using IL-10 and TGF-β: a potential biological immunotherapy for intervertebral disc degeneration in a beagle model, Int. J. Mol. Sci. 15 (2014) 17270–17283.

[20] H. Yang, C. Cao, C. Wu, C. Yuan, Q. Gu, Q. Shi, J. Zou, TGF-βl suppresses inflammation in cell therapy for intervertebral disc degeneration, Sci. Rep. 5 (2015) 13254.

[21] I.Y. Kim, S.J. Seo, H.S. Moon, M.K. Yoo, I.Y. Park, B.C. Kim, B.C. Kim, C.S. Cho, Chitosan and its derivatives for tissue engineering applications, Biotechnol. Adv. 26 (2008) 1–21.

[22] J.C. Antunes, C.L. Pereira, M. Molinos, F. Ferreira-da-Silva, M. Dessi, A. Gloria, L. Ambrosio, R.M. Gonçalves, M.A. Barbosa, Layer-by-layer self-assembly of chitosan and poly(γ-glutamic acid) into polyelectrolyte complexes, Biomacromolecules 12 (2011) 4183–4195.

[23] M.I. Oliveira, S.G. Santos, M.J. Oliveira, A.L. Torres, M.A. Barbosa, Chitosan drives anti-inflammatory macrophage polarisation and pro-inflammatory dendritic cell stimulation, Eur. Cell Mater. 24 (2012) 136–153.

[24] J.N. Barbosa, I.F. Amaral, A.P. Aguas, M.A. Barbosa, Evaluation of the effect of the degree of acetylation on the inflammatory response to 3D porous chitosan scaffolds, J. Biomed. Mater. Res. A 93 (2010) 20–28.

[25] J. Maciel, M.I. Oliveira, E. Colton, A.K. McNally, C. Oliveira, J.M. Anderson, M.A. Barbosa, Adsorbed fibrinogen enhances production of bone- and angiogenic-related factors by monocytes/macrophages, Tissue Eng. Part A 20 (2014) 250–263.

[26] D.P. Vasconcelos, M. Costa, I.F. Amaral, M.A. Barbosa, A.P. Águas, J.N. Barbosa, Development of an immunomodulatory biomaterial: using resolvin D1 to modulate inflammation, Biomaterials 53 (2015) 566–573.

[27] S. Franz, S. Rammelt, D. Scharnweber, J.C. Simon, Immune responses to implants – a review of the implications for the design of immunomodulatory biomaterials, Biomaterials 32 (2011) 6692–6709.

[28] Z.X. Liao, S.F. Peng, Y.C. Ho, F.L. Mi, B. Maiti, H.W. Sung, Mechanistic study of transfection of chitosan/DNA complexes coated by anionic poly(γ-glutamic acid), Biomaterials 33 (2012) 3306–3315.

[29] S.F. Peng, M.T. Tseng, Y.C. Ho, M.C. Wei, Z.X. Liao, H.W. Sung, Mechanisms of cellular uptake and intracellular trafficking with chitosan/DNA/poly(γ-glutamic acid) complexes as a gene delivery vector, Biomaterials 32 (2011) 239–248.

[30] R.M. Gonçalves, J.C. Antunes, M.A. Barbosa, Mesenchymal stem cell recruitment by stromal derived factor-1-delivery systems based on chitosan/poly(γ-glutamic acid) polyelectrolyte complexes, Eur. Cell Mater. 23 (2012) 249–260.

[31] A.P. Cardoso, R.M. Gonçalves, J.C. Antunes, M.L. Pinto, A.T. Pinto, F. Castro, C. Monteiro, M.A. Barbosa, M.J. Oliveira, An interferon-γ-delivery system based on chitosan/poly(γ-glutamic acid) polyelectrolyte complexes modulates macrophage-derived stimulation of cancer cell invasion in vitro, Acta Biomater. 23 (2015) 157–171.

[32] G.Q. Teixeira, A. Boldt, I. Nagl, C.L. Pereira, K. Benz, H.J. Wilke, A. Ignatius, M.A. Barbosa, R.M. Gonçalves, C. Neidlinger-Wilke, A degenerative/pro-inflammatory intervertebral disc organ culture: an ex vivo model for anti-inflammatory drug and cell therapy, Tissue Eng. Part C Methods 22 (2016) 8–19.

[33] C.L. Pereira, J.C. Antunes, R.M. Gonçalves, F. Ferreira-da-Silva, M.A. Barbosa, Biosynthesis of highly pure poly-γ-glutamic acid for biomedical applications, J. Mater. Sci. Mater. Med. 23 (2012) 1583–1591.

[34] S. Vranic, N. Boggetto, V. Contremoulins, S. Mornet, N. Reinhardt, F. Marano, A. Baeza-Squiban, S. Boland, Deciphering the mechanisms of cellular uptake of engineered nanoparticles by accurate evaluation of internalization using imaging flow cytometry, Part Fibre Toxicol. 10 (2013) 2.

[35] Y. Phanse, A.E. Ramer-Tait, S.L. Friend, B. Carrillo-Conde, P. Lueth, C.J. Oster, G.J. Phillips, B. Narasimhan, M.J. Wannemuehler, B.H. Bellaire, Analyzing cellular internalization of nanoparticles and bacteria by multi-spectral imaging flow cytometry, J. Vis. Exp. 64 (2012) 3884.

[36] J.J. MacLean, C.R. Lee, S. Grad, K. Ito, M. Alini, J.C. Iatridis, Effects of immobilization and dynamic compression on intervertebral disc cell gene expression in vivo, Spine 28 (2003) 973–981.

[37] P. Colombier, J. Clouet, O. Hamel, L. Lescaudron, J. Guicheux, The lumbar intervertebral disc: from embryonic development to degeneration, Joint Bone Spine 81 (2014) 125–129.

[38] Z.I. Johnson, Z.R. Schoepflin, H. Choi, I.M. Shapiro, M.V. Risbud, Disc in flames: roles of TNF-α and IL-1β in intervertebral disc degeneration, Eur. Cell Mater. 30 (2015) 104–117.

[39] A. Bertolo, T. Thiede, N. Aebli, M. Baur, S.J. Ferguson, J.V. Stoyanov, Human mesenchymal stem cell co-culture modulates the immunological properties of human intervertebral disc tissue fragments in vitro, Eur. Spine J. 20 (2011) 592–603.

[40] C.L. Korecki, J.J. Costi, J.C. Iatridis, Needle puncture injury affects intervertebral disc mechanics and biology in an organ culture model, Spine 22 (2008) 235–241.

[41] C.L. Pereira, R.M. Gonçalves, M. Peroglio, G. Pattappa, M. D'Este, D. Eglin, M.A. Barbosa, M. Alini, S. Grad, The effect of hyaluronan-based delivery of stromal cell-derived factor-1 on the recruitment of MSCs in degenerating intervertebral discs, Biomaterials 35 (2014) 8144–8153.

[42] J.S. Kim, M.B. Ellman, D. Yan, H.S. An, R. Kc, X. Li, D. Chen, G. Xiao, G. Cs-Szabo, D.W. Hoskin, D.D. Buechter, A.J. Van Wijnen, H.J. Im, Lactoferricin mediates anti-inflammatory and anti-catabolic effects via inhibition of IL-1 and LPS activity in the intervertebral disc, J. Cell. Physiol. 228 (2013) 1884–1896.

[43] R.K. Ponnappan, D.Z. Markova, P.J. Antonio, H.B. Murray, A.R. Vaccaro, I.M. Shapiro, D.G. Anderson, T.J. Albert, M.V. Risbud, An organ culture system to model early degenerative changes of the intervertebral disc, Arthritis Res. Ther. 13 (2011) R171.

[44] S.M. Kim, S.H. Lee, B.R. Lee, J.W. Hwang, Analysis of the correlation among age, disc morphology, positive discography and prognosis in patients with chronic low back pain, Ann. Rehabil. Med. 39 (2015) 340–346.

[45] N. Sasaki, M. Sekiguchi, S. Kikuchi, S. Konno, Anti-nociceptive effect of bovine milk-derived lactoferrin in a rat lumbar disc herniation model, Spine 35 (2010) 1663–1667.

[46] D.A. LaVan, T. McGuire, R. Langer, Small-scale systems for in vivo drug delivery, Nat. Biotechnol. 21 (2003) 1184–1191.

[47] R. Tsaryk, A. Gloria, T. Russo, L. Anspach, R. de Santis, S. Ghanaati, R.E. Unger, L. Ambrosio, C.J. Kirkpatrick, Collagen-low molecular weight hyaluronic acid semi-interpenetrating network loaded with gelatin microspheres for cell and growth factor delivery for nucleus pulposus regeneration, Acta Biomater. 20 (2015) 10–21.

[48] D.R. Pereira, J. Silva-Correia, S.G. Caridade, J.T. Oliveira, R.A. Sousa, A.J. Salgado, J.M. Oliveira, J.F. Mano, N. Sousa, R.L. Reis, Development of gellan gum-based microparticles/hydrogel matrices for application in the intervertebral disc regeneration, Tissue Eng. Part C Methods 17 (2011) 961–972.

[49] X. Yang, X.L. Jin, L. Yao, F.H. Shen, A.L. Shimer, X. Li, Antioxidative nanofullerol prevents intervertebral disk degeneration, Int. J. Nanomed. 9 (2014) 2419–2430.

[50] J.C. Antunes, C.L. Pereira, G.Q. Teixeira, R.V. Silva, J. Caldeira, S. Grad, R.M. Gonçalves, M.A. Barbosa, Poly(γ-glutamic acid) and poly(γ-glutamic acid)-based nanocomplexes enhance type II collagen production in intervertebral

disc, J. Mater. Sci. Mater. Med. (2015), http://dx.doi.org/10.1007/s10856-016-5674-9.
[51] P. Jones, L. Gardner, J. Menage, G.T. Williams, S. Roberts, Intervertebral disc cells as competent phagocytes in vitro: implications for cell death in disc degeneration, Arthritis Res. Ther. 10 (2008) R86.
[52] S.F. Peng, M.J. Yang, C.J. Su, H.L. Chen, P.W. Lee, M.C. Wei, H.W. Sung, Effects of incorporation of poly(gamma-glutamic acid) in chitosan/DNA complex nanoparticles on cellular uptake and transfection efficiency, Biomaterials 30 (2009) 1797–1808.
[53] F.C. Bach, N. Willems, L.C. Penning, K. Ito, B.P. Meij, M.A. Tryfonidou, Potential regenerative treatment strategies for intervertebral disc degeneration in dogs, BMC Vet. Res. 10 (2014) 3.
[54] H.E. Gruber, B. Gordon, C. Williams, J.A. Ingram, H.J. Norton, E.N. Hanley Jr., A new small animal model for the study of spine fusion in the sand rat: pilot studies, Lab. Anim. 43 (2009) 272–277.
[55] J.C. Antunes, R. Tsaryk, R.M. Gonçalves, C.L. Pereira, C. Landes, C. Brochhausen, S. Ghanaati, M.A. Barbosa, C.J. Kirkpatrick, Poly(γ-glutamic acid) as an exogenous promoter of chondrogenic differentiation of human mesenchymal stem/stromal cells, Tissue Eng. Part A 21 (2015) 1869–1885.
[56] A. Prescott, Methods for Treating Joint Pain Using Poly-Gamma-Glutamic Acid, 2006. US20060234192 A1.
[57] T.W. Kim, T.Y. Lee, H.C. Bae, J.H. Hahm, Y.H. Kim, C. Park, T.H. Kang, C.J. Kim, M. H. Sung, H. Poo, Oral administration of high molecular mass poly-gamma-glutamate induces NK cell-mediated antitumor immunity, J. Immunol. 179 (2007) 775–780.
[58] E.H. Kim, Y.K. Choi, C.J. Kim, M.H. Sung, H. Poo, Intranasal administration of poly-gamma glutamate induced antiviral activity and protective immune responses against H1N1 influenza A virus infection, Virol. J. 12 (2015) 160.
[59] T. Uto, T. Akagi, K. Yoshinaga, M. Toyama, M. Akashi, M. Baba, The induction of innate and adaptive immunity by biodegradable poly(γ-glutamic acid) nanoparticles via a TLR4 and MyD88 signaling pathway, Biomaterials 32 (2011) 5206–5212.
[60] T. Akagi, T. Kaneko, T. Kida, M. Akashi, Preparation and characterization of biodegradable nanoparticles based on poly(gamma-glutamic acid) with l-phenylalanine as a protein carrier, J. Control Release 108 (2005) 226–236.
[61] C.H. Chang, Y.H. Lin, C.L. Yeh, Y.C. Chen, S.F. Chiou, Y.M. Hsu, Y.S. Chen, C.C. Wang, Nanoparticles incorporated in pH-sensitive hydrogels as amoxicillin delivery for eradication of *Helicobacter pylori*, Biomacromolecules 11 (2010) 133–142.
[62] Y.H. Lin, C.K. Chung, C.T. Chen, H.F. Liang, S.C. Chen, H.W. Sung, Preparation of nanoparticles composed of chitosan/poly-γ-glutamic acid and evaluation of their permeability through Caco-2 cells, Biomacromolecules 6 (2005) 1104–1112.
[63] A. Corti, M. Franzini, A. Paolicchi, A. Pompella, Gamma-glutamyltransferase of cancer cells at the crossroads of tumor progression, drug resistance and drug targeting, Anticancer Res. 30 (2010) 1169–1181.
[64] E.V. Tchetina, J.A. Di Battista, D.J. Zukor, J. Antoniou, A.R. Poole, Prostaglandin PGE2 at very low concentrations suppresses collagen cleavage in cultured human osteoarthritic articular cartilage: this involves a decrease in expression of proinflammatory genes, collagenases and COL10A1, a gene linked to chondrocyte hypertrophy, Arthritis Res. Ther. 9 (2007) R75.
[65] H. Cho, S. Lee, S.H. Park, J. Huang, K.A. Hasty, S.J. Kim, Synergistic effect of combined growth factors in porcine intervertebral disc degeneration, Connect. Tissue Res. 54 (2013) 181–186.